Subaqueous Explosive Eruption and Welding of Pyroclastic Deposits

Peter Kokelaar and Cathy Busby

Silicic tuffs infilling an ancient submarine caldera, at Mineral King in California, show microscopic fabrics indicative of welding of glass shards and pumice at temperatures >500°C. The occurrence indicates that subaqueous explosive eruption and emplacement of pyroclastic materials can occur without substantial admixture of the ambient water, which would cause chilling. Intracaldera progressive aggradation of pumice and ash from a thick, fast-moving pyroclastic flow occurred during a short-lived explosive eruption of ~26 cubic kilometers of magma in water ≥150 meters deep. The thickness, high velocity, and abundant fine material of the erupted gas-solids mixture prevented substantial incorporation of ambient water into the flow. Stripping of pyroclasts from upper surfaces of subaqueous pyroclastic flows in general, both above the vent and along any flow path, may be the main process giving rise to buoyant-convective subaqueous eruption columns and attendant fallout deposits.

Many volcanoes erupt beneath water, but subaqueous eruptions cannot be observed directly, and their products are difficult to recover and study. Evidence of submarine explosive activity comes from sightings of surface manifestations, such as emergent jets, tsunamis, and water discoloration; appearances of extensive rafts of floating pumice without subaerial sources; seismic and acoustic-signal (*T*-phase) records; and also by inference from the geologic record. Submarine explosive eruptions constitute a significant hazard and have caused loss of life (*1*). Volcanic explosivity beneath water must be hydrostatically suppressed (10 m water = 1 bar), but little is known about possible interactions of erupting magma and ambient water and the depth and pressure controls on the nature and limits of subaqueous explosivity. Recent studies along the Izu-Bonin volcanic arc and associated back-arc rifts, south of Japan, indicate that submarine explosivity can occur at depths of >500 m to perhaps >1800 m (*2*, *3*).

Recognition of hot-state emplacement of subaqueous pyroclastic deposits is fundamental to understanding submarine explosive volcanism, because the evidence of heat retention constrains possible eruption, transport, and depositional processes. The most easily recognized feature indicative of high emplacement temperature in pyroclastic deposits is welding. Welding is hot-state viscous deformation of glassy magmatic particles (pumice clasts and shards). It can occur during emplacement of a tuff in or beneath a depositional boundary layer of a pyroclastic flow (*4*) or immediately following emplacement as a result of loading-compaction (*5*). Welding of rhyolitic glasses apparently requires temperatures >550° to 600°C (*6*), although if water diffuses into hot glass the glass viscosity will be reduced and welding may occur at slightly lower temperatures (*7*).

The possibility of welding of glass fragments under water has long been controversial (*7*–*9*), partly because of the supposition that cold ambient water becomes thoroughly admixed with the fragments during flow or subaqueous eruption (*9*). Theoretical consideration (*7*) suggests that in the case of passage of a subaerial pyroclastic flow into water, formation and expansion of steam at the flow margins may prevent ingress of the ambient water that would cause cooling. The theory may not be applicable, however, as it assumes that a pyroclastic flow moves as a more or less coherent plug, whereas many move as turbulent or laminar particulate streams (*4*). Additionally, there are no clearly documented cases of welding in tuffs at sites where their upper surfaces unequivocally lay below water at the time of deposition (*8*).

In this article we present evidence, from the upper Triassic–lower Jurassic Vandever Mountain tuff at Mineral King in California, for welding of ash-flow tuff in a deep marine environment. Through facies analysis of the enclosing strata, we show that the site of deposition remained in deep water for a considerable time span before and after the tuff was emplaced. We infer that the eruption was subaqueous, and we propose a model that accounts for subaqueous ash-flow eruption and emplacement without substantial interaction of the pyroclasts and ambient water.

P. Kokelaar is in the Department of Earth Sciences, University of Liverpool, Liverpool L69 3BX, United Kingdom. C. Busby is in the Department of Geological Sciences, University of California, Santa Barbara, CA 93106.

Setting and Origin of the Vandever Mountain Tuff

Triassic and lower Jurassic metavolcanic and metasedimentary rocks of the Mineral King area (Fig. 1) record early stages of subduction-related magmatism that continued throughout Mesozoic time along the western edge of North America. The strata now occur as a screen between Cretaceous plutons of the Sierra Nevada batholith and dip vertically to form an east-facing homocline locally complicated by folds and faults. Although the rocks have been metamorphosed at upper greenschist facies, many primary textures and structures are well preserved and, for brevity, we refer to the rocks as volcanic and sedimentary rocks. Present-day stratigraphic thicknesses (Table 1) are probably about half the original value (*10*).

Strata at Mineral King record several episodes of volcanic and tectonic activity

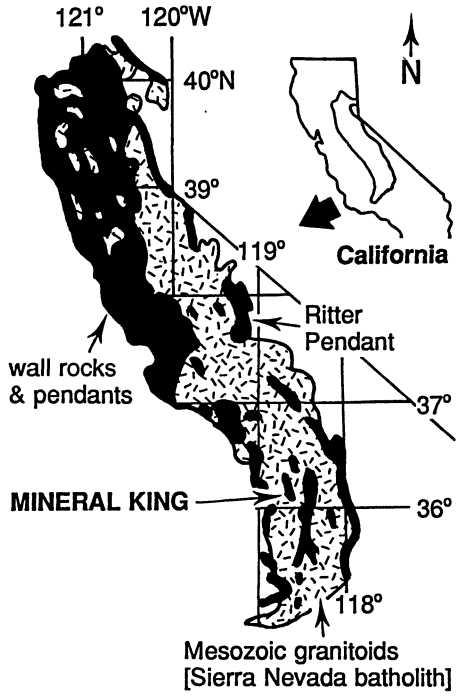

Fig. 1. Location of the Mineral King metavolcanic and metasedimentary rocks in the Sierra Nevada batholith, California.

characterized by submarine caldera-forming eruptions of rhyolitic pumiceous ash-flow tuff (*11*), small-volume eruptions of andesite (*12*), and growth of submarine sedimentary fans and aprons (*13*). These episodes alternated with times of quiescence characterized by deposition of progradational clastic sequences and carbonate in nearshore to shelf environments and fine-grained sediments in relatively deep water (*14*). Rates of tectonic subsidence were high, averaging ~180 m per million years (*14*), and the rocks are inferred to have formed in an arc graben-depression traceable for 1000 km from the Sierra Nevada to Sonora, Mexico (*15*). The Vandever Mountain tuff is the fill and outflow deposit of one of the calderas formed by a submarine explosive eruption of rhyolite.

Evidence for the intracaldera origin of the Vandever Mountain tuff includes: (i) abutment of the thick massive tuff against steep (nondegraded) normal-fault scarps on either side, (ii) offset of strata below the tuff but not above it, demonstrating that subsidence occurred on the bounding normal faults during the eruption, (iii) absence of internal flow-unit boundaries or other forms of tuff stratification, and restriction of subaqueous suspension-fallout deposits to the top, showing that the entire section of massive tuff accumulated rapidly and continuously, (iv) systematic mineralogic variation stratigraphically upward through the massive tuff (Table 1), indicating that eruption involved progressive draw-down of a

Table 1. Summary stratigraphy and sedimentological evidence for marine environment of the Vandever Mountain tuff (*12, 14, 31*). Section is broken into four map units.

Protolith	Sedimentary structures and textures*	Depositional environment and processes†	Basal contacts and thickness‡
		IV. Slate	
Black shale and siltstone, commonly pyritiferous, with minor thin-bedded volcanic-lithic sandstone, rare thin beds of tuff, and very rare thick beds of tuff breccia.	Shales massive or planar-laminated, non-bioturbated; sandstone beds show Bouma turbidite sequences T_{c-e} or T_{d-e} and local basal scour; tuffs planar-laminated or massive; tuff breccias massive to normally graded and indistinctly stratified.	Starved deep-marine basin (*23*), somewhat anoxic, which only occasionally received minor turbidity current incursions and subaqueous fallout of ash, and very rare volcaniclastic debris flows.	Thin beds of black shale are interstratified with uppermost several meters of Vandever Mountain tuff; minimum stratigraphic thickness ~150 m.
		III. Vandever Mountain tuff	
4. Polymictic matrix-supported breccias: up to 25% volcanic and sedimentary rock fragments in a black matrix of very fine grained siliceous material representing remobilized ash (it is identical to finest tuffs in subaqueous fallout successions at Mineral King); blocks 1 to 100 m long enclosed.	Largely disorganized; only minor localized grading or stratification.	Subaqueous debris-flow deposition inferred from: (i) lack of winnowed, clast-supported conglomerates or other evidence of reworking typical of subaerially emplaced debris-flow deposits (*32*) and (ii) loading structures at contact with underlying tuffs, which indicate deposition upon water-saturated ash.	Interstratified with uppermost 5 to 10 m of the tuff and overlies it in a horizon up to 15 m thick along northern 1.5 km of the caldera; locally shows loading-induced interpenetration with underlying tuff, on a scale of meters to tens of meters.
3. Distinctly bedded facies: medium- to thin-bedded lapilli tuffs and coarse-grained tuffs alternate with thin-bedded medium to very fine grained tuffs.	Medium beds commonly graded, show scour-and-fill and rip-up clasts at their bases and small-scale slumps; thin beds very well sorted and planar-laminated; crystal-rich tuffs are normal-graded.	Medium-bedded tuffs deposited from turbidity currents; thin-bedded tuffs deposited from subaqueous fallout and dilute sediment-gravity flows (turbid flows).	Gradational contact with indistinctly bedded facies indicated by local occurrence of thin layers (relatively indistinct, discontinuous, or disrupted) below the contact; 0 to 5 m thick.
2. Indistinctly bedded facies: layers (2 to 30 cm) of tuff breccia, lapilli tuff, and tuff, with extremely gradational upper and lower contacts.	Sorting moderate to poor; layers laterally discontinuous on a scale of meters due to rapid variation in the degree of sorting.	Flow unsteadiness during (relatively low-rate) progressive aggradation or laminar-shear–induced segregation of finer from coarser material along differentially flowing layers in a pyroclastic debris flow.	Gradational contact with underlying massive facies; 0 to 30 m thick.
1. Massive facies: rhyolitic welded pumiceous ash-flow tuff; up to ~50% pumice lapilli, 2 to 20% volcanic and sedimentary lithic lapilli, and 20% phenocrysts (normalized to 0% lithics); K-feldspar to plagioclase ratio and quartz content decrease upward through the deposit; northernmost 2 km encloses megablocks (up to at least 100 m long) and mesobreccias of underlying breccia-sandstone at many stratigraphic levels.	Monotonously massive nonsorted lapilli tuff lacking sedimentary or volcanic interbeds; moderate to intense welding fabrics preserved in strain shadows around intracaldera megablocks; welding-compaction possibly increased away from megablocks, as latter may have caused some chilling.	Monotonous character and absence of stratification with systematic mineralogic variation indicate extremely rapid progressive aggradation during lateral flow; simultaneous shedding of slide megablocks and breccias from northern caldera wall.	Sharp concordant contact with underlying sedimentary rocks; latter are interbedded with small-volume pyroclastic-flow deposits similar in appearance to the Vandever Mountain tuff, suggesting conformity; underlying unit interpreted as caldera floor also forms caldera walls and substrate to outflow tuffs and is source of slide megablocks; 200 to 480 m thick.
		II. Breccia-sandstone	
Lithic tuffaceous sandstones, tuffaceous sandstone, polymictic (volcanic and sedimentary) lithic breccias, rhyolitic lapilli tuffs, and tuffs.	Deposits coarsen northward; coarse nonstratified, nongraded breccias pass southward into stratified graded breccias; medium- to thick-bedded, medium- to coarse-grained sandstones with Bouma turbidite sequences T_{a-c} and erosive loaded bases pass southward into thin- to medium-bedded graded planar-laminated sandstones with nonerosive bases; massive rhyolitic tuff breccias and lapilli tuffs pass southward into thin-bedded lapilli tuffs and planar-laminated tuffs.	Apron of debris shed from the scarp of a normal fault that acted as a conduit for eruptions precursoral to Vandever Mountain tuff eruption (*11*); breccias are deposits of debris flows and high-density turbidity currents; sandstones deposited by turbidity currents; volcaniclastic deposits from pyroclastic or debris flows, turbidites, and subaqueous fallout.	Presence of similar siltstones several tens of meters above and below contact with underlying unit indicative of concordant gradational contact; up to 200 m thick.
		I. Calcareous siltstone-limestone	
Calcareous thin-bedded siltstones, very fine grained sandstones and tuffs, and mudstones.	Tabular laterally continuous beds with nonerosive bases; planar-laminated.	Settling of ash and silt-to-mud-grade terrigenous detritus through the water column onto a limey substrate, and/or extremely dilute (turbid) flow.	Approximately 200 m thick.

*Wave-generated sedimentary structures are absent throughout. †Deposition was entirely below wave base. ‡Present-day thickness.

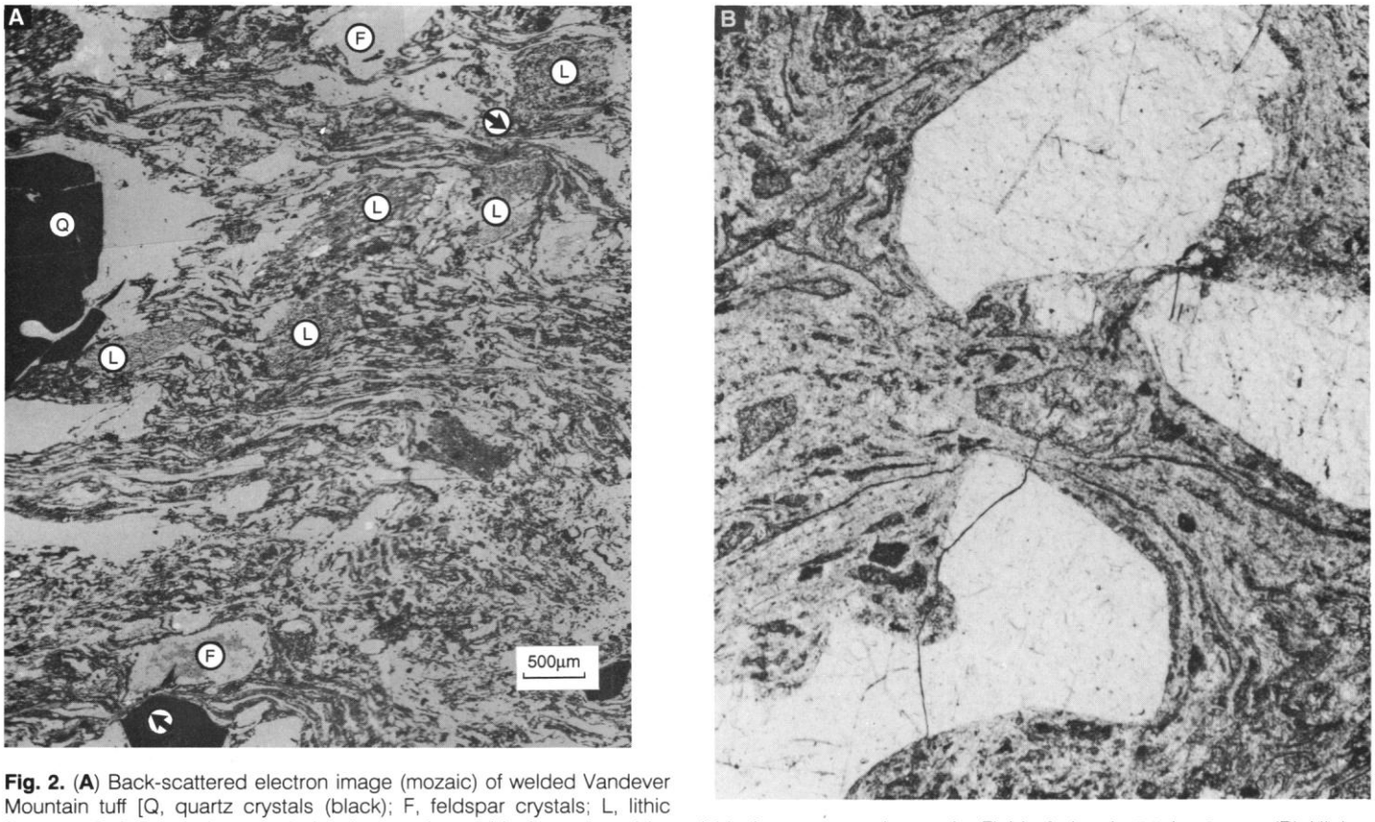

Fig. 2. (**A**) Back-scattered electron image (mozaic) of welded Vandever Mountain tuff [Q, quartz crystals (black); F, feldspar crystals; L, lithic fragments]. Pumice clasts and shards pseudomorphically replaced by crypto- to microcrystalline aggregates of quartz and feldspar, with variable small amounts of sericite, appear white. Arrows indicate sites of pronounced viscous pinching and molding of pumice clasts between lithic fragments and crystals. Field of view is 5.5 by 6 mm. (**B**) Higher magnification view in plane-polarized light, showing viscous attenuation and pinching and molding of pumice clasts between and around quartz crystals. Field of view is 2 by 2.5 mm.

compositionally zoned magma body, and (v) presence in and on top of the tuff of megablocks, commonly >100 m long, derived from the vicinity of the fault-scarp margins. If the caldera width in the dip direction is the same as the strike (outcrop) width, the intracaldera tuff volume would be ~13 km^3, and the original volume of (nonvesiculated) magma erupted can be estimated to have been ~26 km^3. Although a vent for the Vandever Mountain tuff has not been positively identified, the southern fault margin shows features [for example, dikes and phyllic alteration (*11*)] suggestive of a vent there, and there is no indication of any central vent.

The systematic mineralogic variation with height [Table 1 (*11*, *16*)] indicates that the massive, poorly sorted intracaldera tuff accumulated from the base upward by steadily progressive aggradation from a persistent pyroclastic stream rather than from a more chaotic accumulation by upwelling or intrusion (*17*). The occurrence of megablocks (1 m to tens of meters long) in discrete horizons in the tuff, and alignment of the blocks and horizons parallel to paleohorizontal, indicates that debris shed from the caldera-fault scarps was emplaced along successive tuff surfaces formed by and during progressive aggradation. Horizons of dispersed mesobreccia (clasts <1 m) record periodic entrainment and transport of lithic fragments far into the caldera on or just above an aggradation surface. If the ring-fracture vent was <1 km wide, the 7-km minimum diameter of the caldera requires that the pyroclastic material flowed laterally at least several kilometers (*17*).

Evidence for Welding and Submarine Environment

A variety of microscopic textural evidence indicates that the Vandever Mountain tuff is welded (Fig. 2). Abundant magmatic gas bubbles (vesicles) in undeformed pumice clasts commonly form an internal close-packed microtubular fabric, but this fabric tends to collapse in welding, and in longitudinal section the bubbles form a sinuous and locally pinched fibrous texture. Shards formed by fragmentation of highly vesicular magma typically are polycuspate, but welding results in flattening of the cusp forms and development of shard interpenetration and interleaving as the porosity is reduced. Both of these characteristic welding textures are evident in Fig. 2, which shows pronounced viscous flattening and attenuation of pumice clasts and shards attendant with their molding and marked differential compaction around the rigid crystals and lithic fragments.

Attention has recently been drawn to occurrences of flattening of clasts due to syn- or postdiagenetic burial-compaction (*18*), in which early replacement of volcanic glass largely by clay minerals (*19*) was followed by collapse of the resultant aggregates. In such cases, the flattened clasts normally do not show internally a viscous-attenuated microscopic vesicular structure as do welding-compacted pumice clasts, and individual shards are commonly not preserved. The resultant streaky-textured rocks are equivocal in respect of discriminating welding from syn- or postdiagenetic compaction. Among the best preserved welding fabrics in ancient rocks are those in which the glass of pumice clasts or shards has been pseudomorphically replaced by cryptocrystalline to microcrystalline quartz-feldspar aggregates as a result of devitrification [(*20*); as shown in Fig. 2]. It is highly unlikely that glass can be replaced by quartz-feldspar aggregates (devitrified) and then deformed during diagenesis or metamorphism to produce a viscous-attenuated microscopic vesicular structure. Also unlikely

is the possibility that these textures can be produced if the glass is first altered to clay mineral assemblages that then collapse and are then replaced by quartz and feldspar.

The samples shown in Fig. 2 come from a zone of minimal tectonic deformation (strain shadow) adjacent and due to a megablock two-thirds of the way up from the base of the massive facies of the Vandever Mountain tuff (Table 1), toward the north end of the caldera where the tuff is ~250 m thick. Although mesoscopic fabrics of flattened large pumice clasts occur widely (*11*), microscopic welding textures are not preserved in the pervasively cleaved tuff that occurs outside the megablock strain shadows. In intracaldera tuffs in general, welding is typically less intense around the margins of megablocks (*21*), owing to the cooling effect of the inclusions. Thus original welding fabrics that developed away from the blocks, throughout the bulk of the Vandever Mountain tuff, may have been more intense than those shown in Fig. 2.

Evidence of subaerial dissection or fluvial sedimentation is absent from the entire 5.5-km-thick (originally ~11 km) Triassic–lower Jurassic stratigraphic section at Mineral King (Table 1). The Vandever Mountain tuff is underlain and overlain by marine sedimentary rocks with conformable transitional contacts, and characteristics of the uppermost part of the Vandever Mountain tuff also support the interpretation of deposition in a submarine environment. Neither the Vandever Mountain tuff nor its enclosing sedimentary strata (Table 1, units I, II, and IV), show any wave-generated sedimentary structures that would indicate a shallow-marine environment. By analogy with modern marine sediments, this observation suggests that the Vandever Mountain tuff was deposited below wave base, in water depths certainly greater than ~60 m and possibly greater than ~150 to 200 m. The deeper depth is likely if the sediments accumulated in a domain facing open ocean and subject to long-period waves (*22*). Although there is no direct evidence for such conditions at the time of the Vandever Mountain tuff eruption, the Mineral King stratigraphic section as a whole indicates that such a setting was generally prevalent (*14*). Additional evidence is that black pyritous shales and siltstones like those immediately overlying the tuff (>150 m thick; Table 1) typically, although not exclusively, form in deep-water environments (>200 m deep) (*23*). To accommodate the 30-m-thick (proximal) outflow tuffs beneath wave base, the eruption most likely vented in water ≥30 m deeper than the minimum required by the lack of wave-generated sedimentary structures (see above).

Dynamics of Subaqueous Explosive Eruptions

In magmatic explosive eruptions, solid and fluid particles are propelled through and above the vent by the expansion to ambient pressures of exsolved magmatic gases (most commonly and largely water vapor). This behavior characterizes the gas-thrust region of an eruption column (*24*), and in subaerial eruptions air must be incorporated and heated here to reduce the bulk density of the column so as to permit its further wholesale ascent by development of buoyancy [the "convective region" (*24*)]. The mixing of ambient air into the eruption column, which effectively behaves as a fluid, is induced by turbulence and by shear and acceleration of the column-air contacts (Kelvin-Helmholtz and Rayleigh-Taylor instabilities).

Under water, because of the increased pressure, volatile expansion is suppressed relative to subaerial eruptions, and the suppression increases with water depth. However, it seems that development and physical processes of gas-thrust and convective regions may be broadly similar to subaerial counterparts in many respects (*25*). The nature and extent of likely effects due to interactions of magma and ambient water, both in promoting explosivity and in quenching the system, are largely unknown, although from the Vandever Mountain tuff it would appear that the two substances can remain substantially separate.

Because of suppression of magmatic-volatile expansion, the extent of the gas-thrust region of a subaqueous eruption column must be reduced relative to its subaerial counterpart. Thus the facility for early mixing with ambient fluid will be reduced, and capability for development of column buoyancy by magma-water mixing with consequent heat exchange and expansion will also be diminished. With sufficient suppression a column that might otherwise have developed buoyancy may thus remain relatively dense and form a laterally moving high-concentration particulate flow driven by gravity and by pressure from the vent. However, hydrostatic suppression is not essential for development of vent-fed pyroclastic flows, as these can form subaerially, for example, as a consequence of large-scale collapse of a magma chamber roof.

Cashman and Fiske (*25*) presented a model for the evolution of a subaqueous convective eruption column that results from heating and buoyant ascent of water with admixed pyroclasts and produces cold fallout deposits. Our model is complementary and is concerned with erupted material that fails to become incorporated in a convective column and instead flows from the vent to generate a hot laterally moving particulate flow (Fig. 3).

Model for the Vandever Mountain tuff. The welding seen in the Vandever Mountain tuff requires that at least part of the deposit, and probably most of it, aggraded at temperatures ≥500°C. The hot-em-

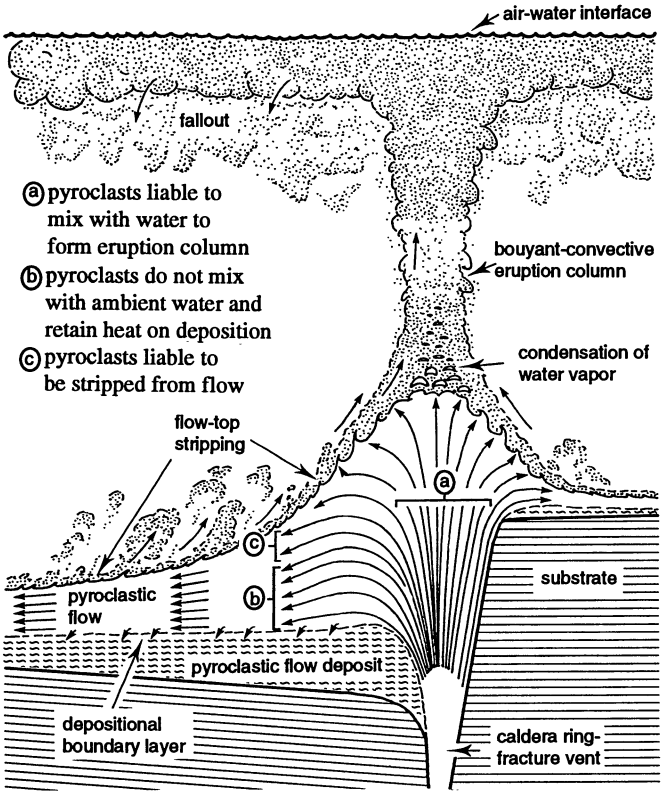

Fig. 3. Schematic diagram illustrating processes of a high-mass-discharge subaqueous explosive eruption. No fixed relative scales are implied.

placed material cannot have mixed significantly with ambient water. Field and petrographic evidence indicates that the deposit aggraded progressively from a particulate flow during a sustained high-mass–discharge explosive eruption in a submarine environment.

When a subaqueous explosive eruption is sustained at a high mass discharge, only the outermost parts of the gaseous particulate flow (column or laterally directed flow) may be able to mix significantly with ambient water, especially near the vent. In depths where the gas-thrust region of a high mass discharge column fails to penetrate the air-water interface, or only just does so, the eruption must involve a laterally moving high-concentration particulate flow that originates directly from the vent. Streamlines from the vent will be like those in a suppressed fountain, and the flow will tend to assume a bell-like shape (Fig. 3), which will be relatively tall in shallower water and flatten out with increasing depth. Given that in near-vent regions the flow is thick and traveling fast (owing to the high mass discharge), and that it is a poorly sorted gas-solids dispersion rich in fine material, it will be impossible for either immediate complete escape of magmatic gases or immediate thorough admixture of the ambient fluid. Because of this, regardless of whether the flow is turbulent or laminar, deflation and wholesale change from a gaseous to an aqueous dispersion cannot occur near to the vent during a sustained high mass discharge subaqueous eruption. In addition, explosive expansion (flashing to steam) of heated ambient water in the outer sheath (boundary layer) of the flow, where mixing with water does occur, should act to prevent incorporation of large volumes of water deep into it. The exclusion of ambient water is similar to that inferred by Kokelaar (*26*) for much smaller scale sustained subaqueous basaltic eruptions. Exclusion of ambient water is only likely to develop effectively during a steadily sustained or smoothly waxing and waning eruption that allows development of a steadily flowing particulate stream. Exclusion of water may be less likely (not impossible) if the gas-thrust region of the eruption column rises substantially above the water surface such that the pyroclastic flow is largely of material that has fallen back into water, albeit close to the vent.

Although most of the fast-moving particulate flow cannot interact with ambient water in near-vent regions, mixing and heat exchange between the magma and water are bound to occur in the outer sheath (boundary layer) of the flow, possibly as a result of turbulence and also by shear and acceleration of the contacts (Fig. 3). Pyroclasts will be removed from the top margins of the laterally moving flow and will ascend with buoyant fluid. We propose that this process, which we refer to as subaqueous pyroclastic-flow stripping, is how warm-water buoyant-convective columns arise. It is the subaqueous counterpart of the subaerial processes whereby convective particulate dispersions arise directly from the gas-thrust region of an eruption column (*24*) as well as from laterally moving pyroclastic flows (*27*), largely as a result of admixture of air with consequent expansion and by sedimentation of large and dense particles. Pyroclastic flows invariably produce some form of overlying buoyant dispersion, which produces fallout deposits (for example, co-ignimbrite ash). Because of the small density difference between erupted particles and water, slower upward velocities of buoyant fluid are required to entrain the particles in subaqueous columns than in subaerial columns (*25*).

For a given erupted volume, the relative amounts of stripped as opposed to flow-emplaced material, and hence the proportion of subaqueous fallout versus flow deposit, will be greater if the eruption is relatively long-lived so that the surface area of the pyroclastic flow is large relative to the underlying volume of flowing material. Conversely, a short-lived high mass discharge eruption will produce a short-lived flow with a relatively low proportion of fallout material. For the Vandever Mountain tuff the limited amount of fallout tuff (Table 1) could be taken to indicate that the amount of material originally suspended was small and hence that the particulate stream was thick and of short duration (perhaps hours or days?). However, an unknown amount of suspended material is likely to have drifted away.

We infer that the Vandever Mountain tuff aggraded rapidly beneath a thick and persistent particulate flow, and, although material escaped as outflow to the south, most flooded into and was ponded within the actively subsiding caldera. For the bulk of the erupted material heat loss was minimal and welding occurred at temperatures >500°C. In consideration of the apparently steady and hot aggradation, combined with likely water depths of ≥150 to 200 m, it seems unlikely that the eruption column ever rose substantially above the water surface.

Toward the end of the eruption, as explosivity diminished, any form of eruptive fountain must have become smaller, and the flow perhaps became unsteady. We interpret the onset of stratification in the uppermost tuffs (indistinctly and distinctly bedded facies; Table 1) as recording this evolution (*28*). The bedded tuffs record fallout of flow-stripped material as well as remobilization of pyroclasts due to slumping of late-deposited material near the vent. Distal and last-deposited fine fallout ash was remobilized in debris flows (polymictic matrix-supported breccias; Table 1).

Conclusions

We suggest that the controversy over the possible occurrence of subaqueous welding of tuff has arisen not because it is rare, but because of the poor preservation potential of diagnostic microstructures and the difficulty of unequivocal demonstration of the paleoenvironment of deposition. Moderate-to-large-volume silicic explosive eruptions mostly occur on continental crust, and those in a submarine setting generally mark a regime of considerable crustal extension. Such regimes are characterized by high heat flow with steep geothermal gradients, intense magmatism, and, commonly, subsequent pronounced crustal shortening. Hence intense hydrothermal alteration [including mineralization (*20*, *29*)], intrusion, metamorphism, and deformation are all to be expected. All of these tend to result in obliteration of microstructures diagnostic of welding. Furthermore, paleoenvironmental interpretation of tuffs is commonly difficult in volcanic terranes where fossils may be rare and depositional environments difficult to compare with standard facies models due to extremely rapid and episodic deposition (*30*).

REFERENCES AND NOTES

1. R. Morimoto, *Bull. Volcanol.* **22**, 151 (1960); _____ and J. Ossaka, *Bull. Earthquake Res. Inst.* **33**, 221 (1953).
2. S. Nagaoka *et al.*, *Rep. Hydrogr. Res. Marit. Saf. Agency (Jpn.)* **27**, 145 (1991); R. S. Fiske, personal communication.
3. J. Gill *et al.*, *Science* **248**, 1214 (1990).
4. M. J. Branney and P. Kokelaar, *Bull. Volcanol.* **54**, in press.
5. R. L. Smith, *U.S. Geol. Surv. Prof. Pap. 354* (1960); J. R. Riehle, *Geol. Soc. Am. Bull.* **84**, 2193 (1973).
6. I. Friedman *et al.*, *J. Geophys. Res.* **68**, 6523 (1963); K. Yagi, *Bull. Volcanol.* **29**, 559 (1966).
7. R. S. J. Sparks *et al.*, *J. Volcanol. Geotherm. Res.* **7**, 97 (1980).
8. R. A. F. Cas and J. V. Wright, *Bull. Volcanol.* **53**, 357 (1991).
9. J. Stix, *Earth-Sci. Rev.* **31**, 21 (1991).
10. An average of 50% shortening perpendicular to cleavage and bedding has been demonstrated for similar strata of the same age in the Ritter roof pendant of the Sierra Nevada, 130 km north of Mineral King, see O. T. Tobisch and R. S. Fiske, *Geol. Soc. Am. Bull.* **87**, 1411 (1976).
11. C. J. Busby-Spera, *J. Geophys. Res.* **89**, 8417 (1984).
12. _____, *J. Volcanol. Geotherm. Res.* **27**, 43 (1986).
13. _____, *J. Sed. Petrol.* **55**, 376 (1985).
14. _____, in *Tectonics and Sedimentation Along the California Margin*, S. Bachman and J. Crouch, Eds. (Society of Economic Paleontologists and Mineralogists, Los Angeles, 1984), pp. 135–156.
15. C. J. Busby-Spera, *Geology* **16**, 1121 (1988); _____ *et al.*, *Geol. Soc. Am. Spec. Pap.* **255**, 325 (1990).
16. C J. Busby-Spera, thesis, Princeton University, Princeton, NJ (1983).

17. Cas and Wright (*8*) suggested that intracaldera tuffs do not result from pyroclastic flow and hence are not true pyroclastic flow deposits. They do not explain the processes they envision, but in this situation pyroclastic emplacement without some form of lateral flow is clearly impossible, even in near-vent locations.
18. M. J. Branney and R. S. J. Sparks, *J. Geol. Soc. London* **147**, 919 (1990).
19. For example, halloysite, smectites, sericite, montmorillonite, kaolinite, and illite.
20. R. L. Allen, *Econ. Geol.* **83**, 1424 (1988).
21. P. W. Lipman, *Geol. Soc. Am. Bull.* **87**, 1397 (1976).
22. L. Draper, *Marine Geol.* **5**, 133 (1966); P. D. Komar, *J. Sed. Petrol.* **44**, 169 (1974); B. Butnam *et al.*, *J. Geophys. Res.* **84**, 1182 (1979).
23. See K. T. Pickering *et al.*, *Deep Marine Environments* (Unwin Hyman, London, 1989).
24. R. S. J. Sparks, *Bull. Volcanol.* **48**, 3 (1986).
25. K. V. Cashman and R. S. Fiske, *Science* **253**, 275 (1991). These authors described a fallout deposit resting above a coeval hot-emplaced (~450°C) flow deposit, which we suggest is most likely to have formed from the material that would not be incorporated into the convective column above the vent.
26. P. Kokelaar, *Bull. Volcanol.* **48**, 275 (1986), figure 4. A bell-shaped exclusion zone postulated to occur above the vent was referred to in that case as a "cupola of steam," because the explosivity involves bulk incorporation of water in the eruptive conduit, so that the gas of the erupted dispersion is dominated by (nonmagmatic) steam; see P. Kokelaar, *J. Geol. Soc. London* **140**, 939 (1983).
27. P. D. Rowley *et al.*, *U.S. Geol. Surv. Prof. Pap. 1250* (1981), p. 489.
28. Compare with R. S. Fiske and T. Matsuda, *Am. J. Sci.* **262**, 76 (1964).
29. H. Ohmoto and B. J. Skinner, *Econ. Geol. Monogr.* **5**, 1 (1983).
30. P. Kokelaar, *Geol. Soc. Am. Bull.*, in press.
31. C. J. Busby-Spera and J. Saleeby, *Geologic Guide to the Mineral King Area, Sequoia National Park, California* (Society of Economic Paleontologists and Mineralogists, Los Angeles, 1987).
32. T. G. Gloppen and R. J. Steel, *Soc. Econ. Paleontol. Mineral. Spec. Publ.* **31**, 49 (1981).
33. Supported by a NATO collaborative research grant 910549 and NSF grant EAR9018606 (to C.B.). We are grateful to G. Lloyd for assistance with production of the SEM image and to M. J. Branney, R. V. Fisher, S. Self, and R. S. J. Sparks for reviews of a draft of the article.

RESEARCH ARTICLES

Deficient Hippocampal Long-Term Potentiation in α-Calcium-Calmodulin Kinase II Mutant Mice

Alcino J. Silva, Charles F. Stevens, Susumu Tonegawa, Yanyan Wang

As a first step in a program to use genetically altered mice in the study of memory mechanisms, mutant mice were produced that do not express the α-calcium-calmodulin–dependent kinase II (α-CaMKII). The α-CaMKII is highly enriched in postsynaptic densities of hippocampus and neocortex and may be involved in the regulation of long-term potentiation (LTP). Such mutant mice exhibited mostly normal behaviors and presented no obvious neuroanatomical defects. Whole cell recordings reveal that postsynaptic mechanisms, including *N*-methyl-D-aspartate (NMDA) receptor function, are intact. Despite normal postsynaptic mechanisms, these mice are deficient in their ability to produce LTP and are therefore a suitable model for studying the relation between LTP and learning processes.

Long-term potentiation (LTP) is an electrophysiological manifestation of a long-lasting increase in the strength of synapses that have been used appropriately (*1*). Although LTP has been studied as a mechanism responsible for some types of learning and memory, the actual evidence for this hypothesis is not extensive. The main support for LTP as a memory mechanism is the observation that pharmacological agents that block hippocampal glutamate receptors of the *N*-methyl-D-aspartate (NMDA) class and thus prevent the induction of LTP also impair spatial learning in rodents (*2*). The problem with this evidence is that blocking NMDA receptors disrupts synaptic function and thus potentially interferes with the in vivo computational ability of hippocampal circuits. Perhaps the failure of learning results not from the deficit in LTP but simply from some other incorrect operation of hippocampal circuits that lack NMDA receptor function.

We have adopted a strategy for the study of the mechanisms of mammalian memory, designed to address the relation of LTP to learning; we have produced mice with mutations in individual enzymes likely to be involved in the regulation of candidate memory mechanisms, such as LTP. These specific mutations were made with the use of gene targeting (*3*). As a first step in this program, we report studies on a strain of mutant mice that do not express the α isoform of calcium-calmodulin–dependent protein kinase type II (α-CaMKII). This enzyme is neural-specific and is present presynaptically and appears abundantly adjacent to the postsynaptic membrane at synapses that express LTP (*4*, *5*). Calmodulin (CaM) loaded with calcium (Ca^{2+}) activates this enzyme and induces its autophosphorylation. Once autophosphorylated, the CaMKII holoenzyme no longer requires Ca^{2+} or CaM for activity. This switch-like mechanism can maintain the enzyme in an active state beyond the duration of the activating Ca^{2+} signal (*6*) and has been invoked in learning models (*7*). Pharmacological experiments have implicated this holoenzyme in the induction of LTP (*8*, *9*). Although postsynaptic mechanisms seem normal in the CA1 hippocampal region of these mutant mice, we find little or no LTP. We thus have a strain of mice that should be suitable for studying the behavior implications of normal synaptic transmission but deficient LTP. In the accompanying paper we show that these mutant mice are impaired in performing a spatial-learning task (*10*).

α-CaMKII mutant mice. In order to produce mice with a mutation in the α-CaMKII locus, we constructed the plasmid p23 (Fig. 1A) which contains a 6.1 kilobase (kb) mouse genomic α-CaMKII sequence that is disrupted by insertion of a neomycin-resistance gene (*neo*) from the plasmid *pgk-neo* (*11*). The insertion is within the α-CaMKII exon encoding most of the regulatory domain, and the inserted sequence replaced a 130-bp mouse genomic sequence flanked by a pair of Sph I sites; the expression product of the 130-bp sequence includes the entire inhibitory domain and five amino acids in the amino end of the calmodulin-binding domain (*12*). We transfected the linealized (Fig. 1A) p23 plasmid into E14 embryonic stem (ES) cells (*13*) by electroporation (*13*) and isolated 150 (*neo*) colonies, of which two (E14-20 and E14-84) were shown by Southern blotting analysis to harbor a homologously integrated plasmid.

We injected the E14-20 ES cells into C57B1/6J blastocysts and transferred the blastocysts into pseudo-pregnant mothers. Twelve male chimeric mice were born; they were bred with BALB/c females. Hybridization blot analysis (Southern) of tail DNA from the offspring of the chimeric males,

A. J. Silva and S. Tonegawa are at the Howard Hughes Medical Institute, Center for Cancer Research and Department of Biology, Massachusetts Institute of Technology, Cambridge, MA 02139. C. F. Stevens and Y. Wang are at the Howard Hughes Medical Institute, Salk Institute, 10010 North Torrey Pines Road, La Jolla, CA 92037.